communications biology

Article

https://doi.org/10.1038/s42003-024-06673-w

Disrupted brain functional connectivity as early signature in cognitively healthy individuals with pathological CSF amyloid/tau

Check for updates

Abdulhakim Al-Ezzi[1] ✉, Rebecca J. Arechavala[2], Ryan Butler[1], Anne Nolty[3], Jimmy J. Kang[4], Shinsuke Shimojo[5], Daw-An Wu[5], Alfred N. Fonteh[1], Michael T. Kleinman[2], Robert A. Kloner[1,6] & Xianghong Arakaki[1] ✉

Alterations in functional connectivity (FC) have been observed in individuals with Alzheimer's disease (AD) with elevated amyloid (*Aβ*) and tau. However, it is not yet known whether directed FC is already influenced by A*β* and tau load in cognitively healthy (CH) individuals. A 21-channel electroencephalogram (EEG) was used from 46 CHs classified based on cerebrospinal fluid (CSF) *Aβ* tau ratio: pathological (CH-PAT) or normal (CH-NAT). Directed FC was estimated with Partial Directed Coherence in frontal, temporal, parietal, central, and occipital regions. We also examined the correlations between directed FC and various functional metrics, including neuropsychology, cognitive reserve, MRI volumetrics, and heart rate variability between both groups. Compared to CH-NATs, the CH-PATs showed decreased FC from the temporal regions, indicating a loss of relative functional importance of the temporal regions. In addition, frontal regions showed enhanced FC in the CH-PATs compared to CH-NATs, suggesting neural compensation for the damage caused by the pathology. Moreover, CH-PATs showed greater FC in the frontal and occipital regions than CH-NATs. Our findings provide a useful and non-invasive method for EEG-based analysis to identify alterations in brain connectivity in CHs with a pathological versus normal CSF *Aβ*/tau.

Alzheimer's disease (AD) is a neurological disorder in which progressive neurodegeneration and synaptic dysfunction result in impairments in a range of cognitive domains. With the continual rise of the global population and life expectancy, it is anticipated that the prevalence of neurocognitive disorders or dementia will experience a substantial surge, reaching an estimated 74.7 million individuals by 2030 and more than 131.5 million by 2050 worldwide[1,2]. Recent research reported early impairments in executive functions and memory among individuals afflicted with *Aβ* and/or tau pathologies[3–5]. These findings provide validation for the notion that executive functions and episodic memory[6–8] are indeed affected during the initial stages of AD, primarily due to the alteration or pathology of the frontal and temporal cortices[9,10]. More specifically, inhibitory abilities[11], attentional processes[12,13], and visuospatial functions[14] appear to be particularly compromised. A defining feature of the progression of AD is the reduction in *Aβ* protein (resulting in low levels of CSF amyloid-*β* (*Aβ*) and the rise in neuronal degeneration biomarkers (such as increased levels of CSF total tau and phosphorylated tau) in individuals with AD. The reduction in CSF *Aβ* levels seems to occur in the early progression of AD, becoming apparent more than twenty years before the onset of any clinical symptoms[15]. In individuals with AD or those who are at risk of developing AD, the amyloid-*β*-to-tau ratio is often low, indicating an accumulation of *Aβ* plaques and/or tau tangles in the brain[6,16,17]. Lei Wang et al, found that lower CSF *Aβ*42 levels and higher tau/*Aβ*42 ratios were strongly correlated with a reduction in hippocampal volume and indicators of progressive atrophy of the cornu ammonis subfield in pre-clinical AD individuals, but not cognitively healthy (CH) individuals[18]. Compared to the *Aβ*42 and/or

[1]Department of Neurosciences, Huntington Medical Research Institutes, Pasadena, CA, USA. [2]Department of Environmental and Occupational Health, Center for Occupational and Environmental Health (COEH), University of California, Irvine, CA, USA. [3]Fuller Theological Seminary, Pasadena, CA, USA. [4]The Hill Medical Corporation, Pasadena, CA, USA. [5]The Division of Biology and Biological Engineering, California Institute of Technology, Pasadena, CA, USA. [6]Department of Cardiovascular Research, Huntington Medical Research Institutes, Pasadena, CA, USA. ✉e-mail: hakim.alezzi@hmri.org; xianghong.arakaki@hmri.org

tau, the *Aβ*42/tau ratio demonstrated greater sensitivity in detecting presymptomatic AD and distinguishing it from frontotemporal dementia[19]. Consequently, it is plausible that *Aβ*42/tau ratio may serve as a sensitive biomarker in detecting the earliest stages of preclinical AD compared to individual biomarkers. Preclinical investigations offer robust evidence supporting functional connectivity as a probable intermediary mechanism linking *Aβ* to tau secretion and accumulation[20]. Despite the significant research dedicated to unraveling AD pathogenesis, there is currently a lack of sensitive, specific, reliable, objective, and easily scalable biomarkers or endpoints to guide clinical trials and facilitate early risk detection in clinical settings.

Several large prospective studies attempt to characterize the early diagnostic criteria in people at risk of developing AD. These assessments include pathological markers (both Beta Amyloid (*Aβ*) and tau pathologies)[21], neuropsychological scores (Montreal Cognitive Assessment (MoCA) and Mini-Mental State Examination (MMSE))[22], neuroimaging (Magnetic resonance imaging (MRI), Magnetoencephalography (MEG), and electroencephalogram (EEG)[23], and heart rate variability (HRV)[24]. EEG Brain connectivity, MRI brain structures, neuropsychological assessments, and HRV are intricately correlated measures that can predict early AD pathology. For example, a recent examination of HRV from the Multi-Ethnic study of atherosclerosis revealed a correlation between higher HRV and superior cognitive function across various cognitive domains[25]. We previously reported a significant association between high resting HR and less negative alpha event related resynchronization (ERD) during Stroop testing in individuals with pathological *Aβ*/tau, compared with those with normal *Aβ*/tau[26]. These findings prompt further investigation into brain connectivity involved with pathological *Aβ*/tau presence during task-switching tasks. Therefore, we aim to integrate brain activity, neuropsychology, and HRV assessments in this study to facilitate early detection of AD risks, understand disease mechanisms, and ultimately help improving outcomes for individuals affected by AD by addressing the multifaceted nature of the disease.

The abnormality of brain connectivity measured by MRI in regions with early *Aβ*-burden (e.g., default mode network (DMN) has been shown when *Aβ* fibrils just start to accumulate[27]. However, this abnormality has not been reported or tested in EEG investigations to our knowledge. Both *Aβ* and tau pathologies have been shown to impact brain network's structural and FC[28]. Abnormal FC has been consistently identified in the early stages of AD before the appearance of clinical symptoms or brain structural changes[29]. For instance, a recent study has achieved 90% accuracy in classifying brain *Aβ* and tau pathology in subjective cognitive decline from mild cognitive impairment (MCI) individuals using EEG coherence[30]. FC studies have found that abnormal cerebrospinal fluid (CSF) levels of phosphorylated-tau and *Aβ* in early AD are linked with disrupted cortical networks involving the anterior and posterior cingulate cortex, and temporal and frontal cortices[31]. We previously reported that ERD increased in CH with pathological *Aβ* tau ratio (CH-PATs)[32], compared to CH with normal *Aβ* tau ratio (CH-NATs) in alpha band. Using regional interconnectivity methods, a previous study found that the temporal and frontal regions' connection is a characteristic pattern for the pathological transition of normal to MCI and the density of edges in these networks is a differential pattern between HC and MCI[33]. The decreased patterns of regional hemispheric interconnectivity in the metabolic network rely on the pathology severity[33]. Therefore, EEG can be a promising, diagnostic, noninvasive, high temporal resolution method, which is a cost-effective biomarker and easily accessible to track and predict the severity of cognitive dysfunction in degenerative diseases. As memory (predominantly localized in the temporal region) and executive functions (mainly associated with the frontal region) are the two sensitive cognitive activities that were abnormal in early AD[9,10], it will be compelling to study frontal and temporal FC in the early stage of AD spectrum.

In the present study, we aimed to: (1) compare effective connectivity (EC) between CH-NATs and CH-PATs during task switching, and explore the potential contribution of task difficulty levels; (2) study the links between EC and Neuropsychological measures, structural MRI brain volumes, and HRV.

Results

Participant characteristics

The demographic and clinical characteristics of our subjects have been reported in our previous work[32]). The participants' age in CH-PATs and CH-NATs were comparable and both groups also had similar educational levels, with mean years of education. There were no differences in cognitive reserve (CR) and intelligence quotient (IQ) scores between CH-NATs and CH-PATs.

Behavioral analysis

The difference between the accuracy (ACC) and reaction time (RT) scored under the effect of trial types (repeat or switch) was notable with a significantly improved RT ($p < 0.0001$) and ACC ($p = 0.048$) during repeat trials than during switch trials. In addition, the results of this study showed no significant differences in group × trial type interaction in RT, $F(1, 108) = 0.0001$, $p = 0.991$ and ACC, $F(1, 108) = 0.003$, $p = 0.960$ between the two groups of all CH-PAT and CH-NAT participants. A comparison of the main effect of trial types and group × trial between CH-NATs and CH-PATs was reported previously in our work[32].

EEG power spectral density

The comparison of the normalized alpha power in resting-state and task-switching at the five regions in the CH-PATs and CH-NATs is shown in Fig. 1. The CH-NATs showed significantly stronger spectral power of task-switching alpha at temporal, parietal, and occipital electrodes when compared to CH-PATs ($p < 0.0001$), ($p = 0.0005$ and $p < 0.0001$), respectively as shown in (Fig. 1a, b). On the contrary, there were no significant differences between CH-PATS and CH-NATs in frontal or central power. In the resting state, there were no significant differences in alpha power changes between all brain regions (Fig. 1b, d).

The mean partial directed coherence (PDC) FC pattern of CH-PATs and CH-NATs were shown in Fig. 2a, b, respectively, and we qualitatively observed that the main difference between the two groups was that CH-PATs patients exhibited much more and much weaker long-range connections from left and right temporal cortices than CH-NATs. Specifically, compared with the CH-NATs group (0.135 ± 0.017), the averaged information flow in the alpha frequency of CH-PATs was enhanced in the frontal regions during task switching processing (0.223 ± 0.014); $t(44) = 18.06$, $p < 0.0001$. On the contrary, CH-NATs showed increased information flow from temporal region (0.187 ± 0.016) compared to CH-PATs (0.09 ± 0.015), $t(44) = 21.06$, $p < 0.001$. On the contrary, central, parietal, and occipital regions did not show any significant differences between CH-NATs and CH-PATs. It is also interesting to note that resting-state EC showed a significant difference between CH-NATs and CH-PATs only in the occipital cortex (0.082 ± 0.03), (0.105 ± 0.036), $t(44) = 2.36$, $p = 0.023$ as shown in Fig. 2c, d. Differences in brain connectivity (Switching task connectivity values - Resting state connectivity values) were calculated across five distinct brain regions (Fig. 2e, f). Results revealed differences between CH-NATs and CH-PATs in frontal ((0.036 ± 0.041), (0.084 ± 0.037), $t(44) = 6.985$, $p < 0.0001$) and temporal ((0.072 ± 0.039),(-0.028 ± 0.027), $t(44) = 10.21$, $p < 0.0001$)), while no differences were observed in the parietal, occipital, or central regions.

To validate the outcomes concerning directed connectivity as measured by PDC, we employed multiple functional phase connectivity methodologies, including Weighted Phase Lag Index (wPLI) and Phase locking value (PLV). Although FC and EC can be associated, they estimate distinct characteristics of brain interactions, and the presence of one does not inherently imply the presence of the other. During task-switching, wPLI results showed that CH-PATs demonstrated significantly higher phase connectivity in frontal and central regions (Supplementary Fig. 1). In addition, PLV analysis showed decreased phase coherence in frontal and occipital regions (Supplementary Fig. 2). Detailed results, including

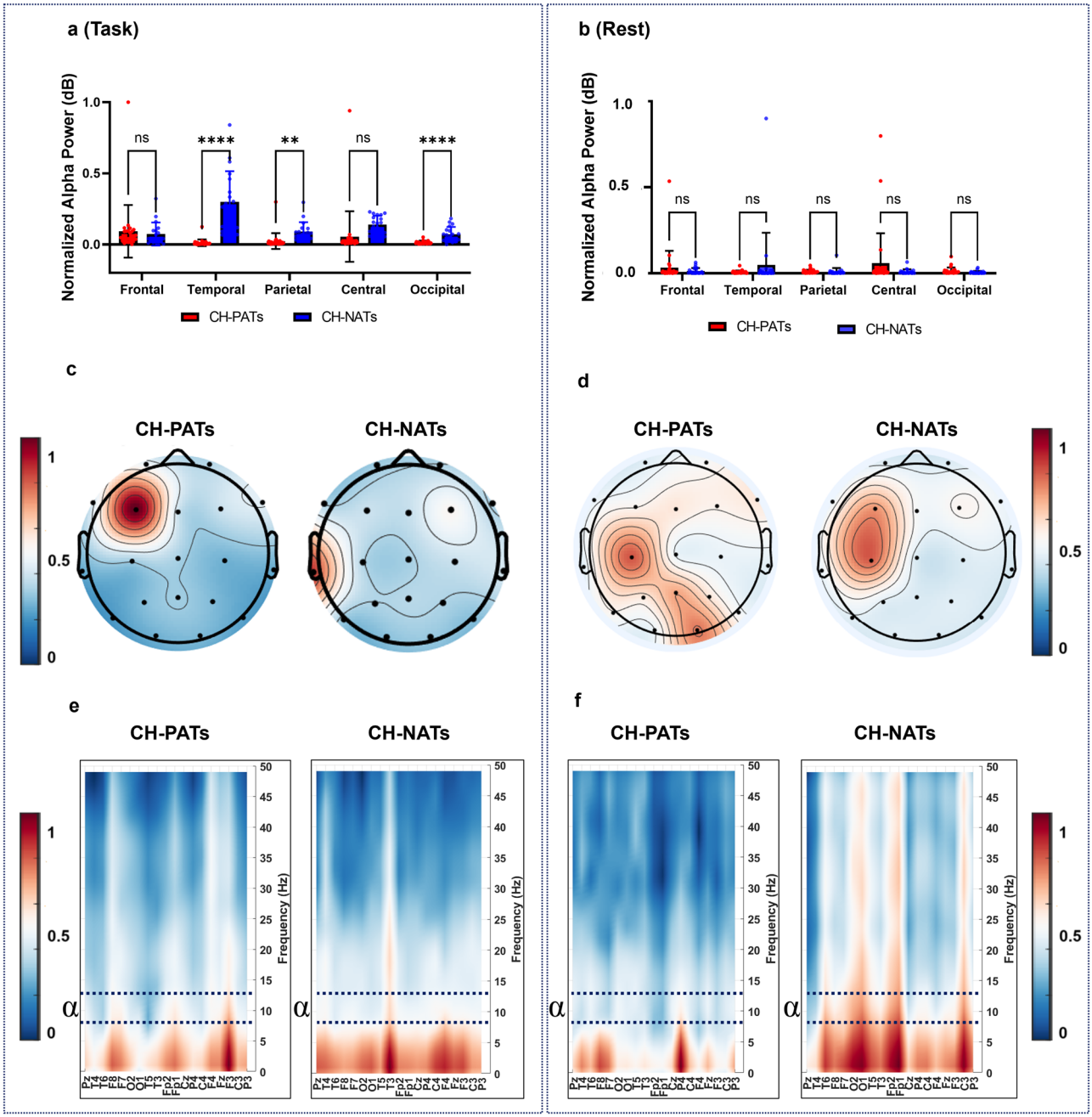

Fig. 1 | Mean normalized absolute power spectral density (PSD) in CH-PATs and CH-NATs. a, **b** A group comparison between CH-PATs and CH-NATs using *t*-test in different brain regions (Frontal, temporal, parietal, central, occipital) within the range (200–550 ms), where 0 ms is the onset of the stimulus during task switching and resting-state, respectively. **c**, **d** Shows the avereged topographical distribution of alpha power in CH-PATs and CH-NATs during task switching and resting-state, respectively. **e**, **f** Shows the mean normalized absolute PSD for all electrodes in the frequency domain (0–50Hz) for CH-NATs and CH-PATs during the switching task and resting state. Frequency bands are decomposed into the following: delta (0.4–4 Hz), theta (4.1–8 Hz), alpha (8.1–12 Hz), and beta (12.1–30 Hz). $^{*}P < 0.05$, $^{**}P < 0.01$, $^{***}P < 0.001$.

additional analyses and comparisons utilizing wPLI and PLV algorithms, are presented in this manuscript's supplementary file.

Task difficulty

To examine the potential contribution of task difficulty level to the EC differences, we selectively compared connectivity between "good performers" in CH-PATs and "bad performers" from CH-NATs to bring down the potential differences and check if the frontal and temporal EC differences remained. Task difficulty was determined through the calculation of performance indicators, namely ACC or RT, and brain connectivity. In this context, the ACC results demonstrated a significant difference between CH-NATs (0.79 ± 0.13) and CH-PATs (0.96 ± 0.03) with $p < 0.0001$. Similarly, the results indicated that CH-NATs showed a significant increase in RT (1743.63 ± 265.6) compared to CH-PATs (1218.47 ± 167.66) with $p < 0.0001$. For this condition, we sorted the EC based on the ACC and RT data (i.e., low-vs-high-connectivity) and constructed a statistical analysis between CH-PATs and CH-NATs. For instance, using EC based on the ACC classification, the CH-PATs showed increased frontal connectivity (0.22 ± 0.02) compared to CH-NATs (0.131 ± 0.02) with $p = 0.0009$. Additionally, the CH-PATs showed decreased temporal connectivity (0.09 ± 0.02) compared to CH-NATs (0.187 ± 0.006) with $p < 0.0001$. Furthermore, using EC based on the RT classification, the CH-PATs showed

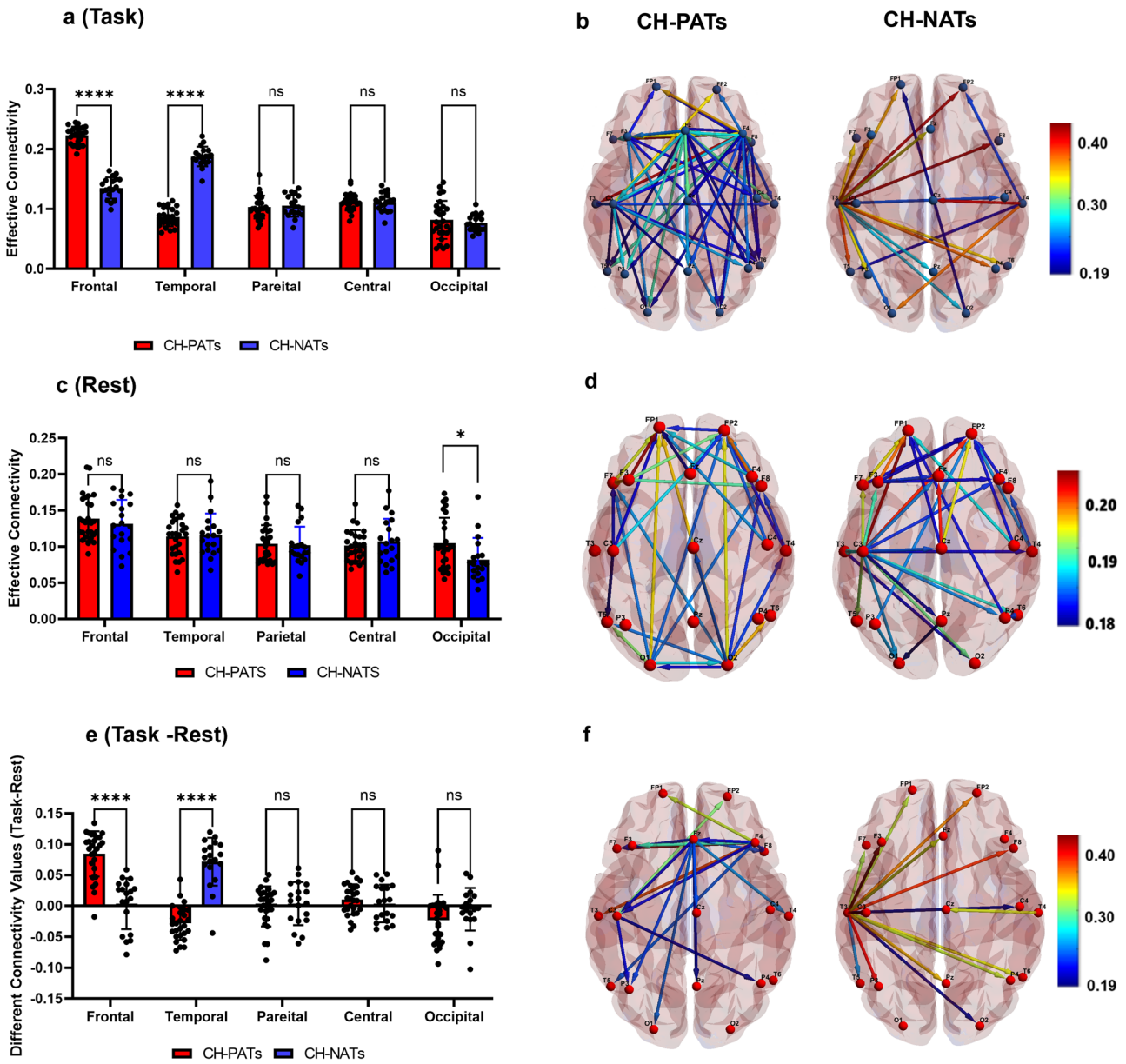

Fig. 2 | The averaged brain connectivity (measured by PDC) at the sensor level. Representation of the functional networks as graphs in the Alpha frequency band at stimuli time (200–550 ms) after the onset of the stimulus. PDC from an area *i* to *j* is represented by an arrow. **a**, **c**, **e** Group connectivity comparison between CH-PATs and CH-NATs during task switching, resting state, and the differences between task switching and resting (Task-rest), respectively in the alpha band. **b**, **d**, **f** The directed connectivity of the CH-PATs (left) and CH-NATs (right) during task switching, resting state, and the differences between task switching and resting (Task-rest), respectively in the alpha band. The brain regions are graphically represented with connections depicting causal influence at (200–550 ms). The brain surface templates we used to visualize these connections in Fig. 2 are primarily generated from a commonly used template known as MNI/Talaraich (ICBM152).

increased frontal connectivity (0.22 ± 0.01) compared to CH-NATs (0.13 ± 0.02) with $p = 0.0008$. The CH-PATs showed decreased temporal connectivity (0.09 ± 0.02) compared to CH-NATs (0.188 ± 0.012) with $p < 0.0001$. This rigorous comparative analysis supported that the EC differences are independent of task difficulty levels. Figure 3 illustrates mean scores for task difficulty based on ACC and RT classifications for the color-Word (cW) test.

Functional connectivity and neuropsychological and cognitive reserve analysis

Supplementary Table 1 presents several correlations between task-switching brain connectivity in temporal and frontal brain regions and different neuropsychological tests (i.e., processing speed, working memory, and executive functions) between CH-NATs and CH-PATs. Processing speed tests were used to assess the ability to process information rapidly. The higher the score, the more time it has taken, and the worse the performance. Executive function and working memory tests can provide an estimation of a wide range of skills (i.e., working memory and organization). The higher the score, the more time it has taken, and the better the performance. While CH-PATs showed greater scores in performance in speed processing tests, CH-NATS showed a better performance in executive function and working memory tests. Also, the present study aimed to investigate the relationship between cognitive reserve (CR) and parietal connectivity in two groups, CH-NATs and CH-PATs. Our findings revealed a significant negative correlation between CR and parietal connectivity in the CH-NATs group ($r = -0.61$, $p = 0.030$), as shown in Fig. 4. This suggests that individuals with higher CR tend to exhibit lower parietal connectivity in this group. However, in

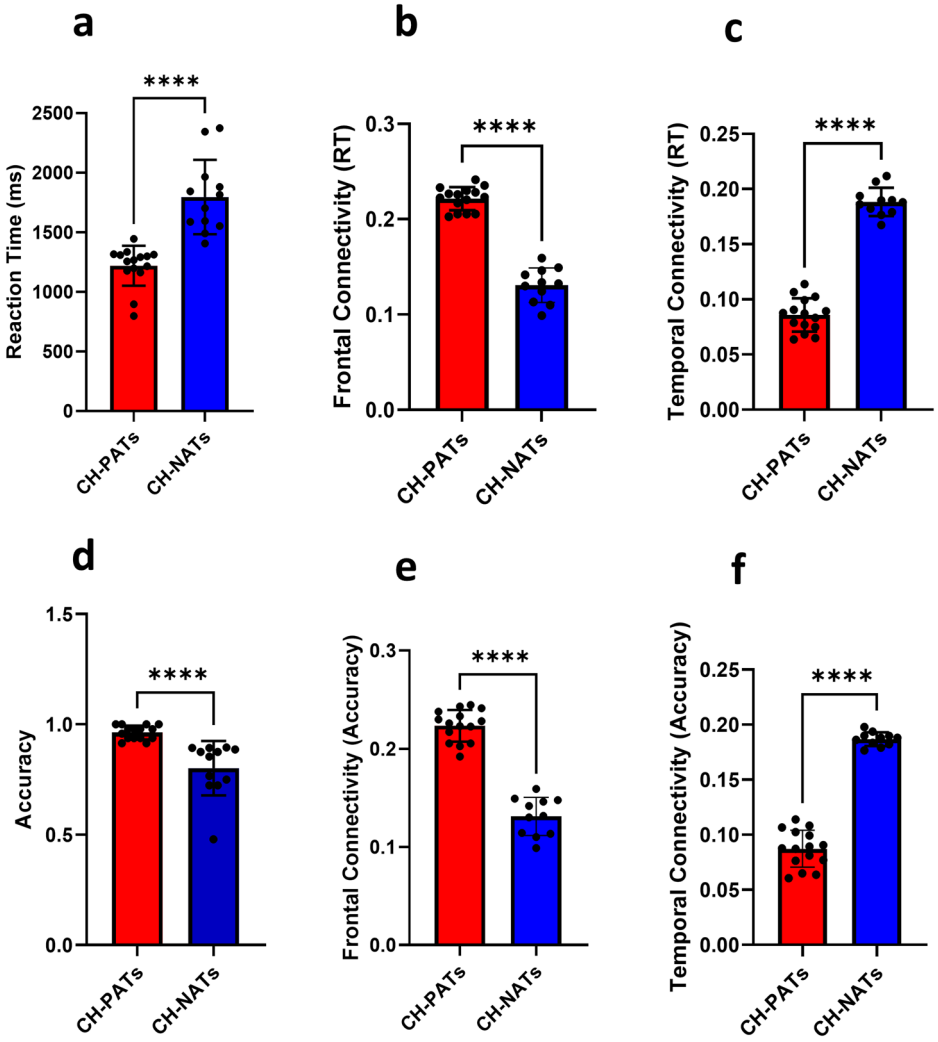

Fig. 3 | Task difficulty and behavioral responses of task switching. a The Reaction Time (RT) was different between CH-NATs and CH-PATs. The values represent the best 50% performance of RT (lowest RT values) in CH-PAT participants and the worst 50% performance (Highest RT values) in CH-NATs during high-load color-word switch trials. The comparison was performed between the two groups for frontal (**b**) and temporal (**c**) connectivity for the same participants. **d** The ACC was significantly different between CH-NATs and CH-PATs. The values represent the good 50% performance of ACC scores (highest ACC values) in CH-PATs and the worst 50% performance (lowest ACC values) in CH-NATs during high-load color-word switch trials. The comparison was performed between the two groups for frontal (**e**) and temporal (**f**) connectivity for the same participants using a parametric *t*-test. $^{*}p < 0.05$, $^{**}p < 0.01$, $^{***}p < 0.001$, $^{****}p < 0.0001$.

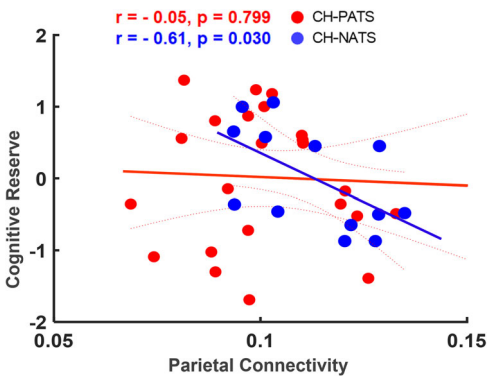

Fig. 4 | Scatterplots with Spearmen correlation represent the relationship between CR and frontal connectivity in CH-NATs (blue scatters) and CH-PATs (red scatters) groups. A linear regression model was used to estimate the coefficients of linear correlations (Confidence Intervals = 0.95) that relate a set of predictor variables to a response variable.

contrast, the CH-PATs group did not show any differences in CR and parietal EC.

Functional connectivity and MRI brain volumes

In the CH-PATs group, significant negative correlations were observed during task switching between temporal EC and several brain volumetrics: Fusiform Right Side Volume ($r = -0.42$, $p = 0.043$), Hippocampal Occupancy Score (HOC) Norm Percentile ($r = -0.46$, $p = 0.023$), and Fusiform Asymmetry Norm Percentile ($r = -0.41$, $p = 0.049$) as shown in Fig. 5. However, CH-NATs did not show significant correlations between temporal EC and the same regions. Moreover, CH-NATs showed significant correlations between temporal EC and Entorhinal Cortex Asymmetry Norm Percentile ($r = -0.67$, $p = 0.013$), Fusiform Left Percent Of intracranial volume (ICV) ($r = -0.58$, $p = 0.041$), and Fusiform Asymmetry Norm Percentile ($r = -0.67$, $p = 0.015$). Additional correlations between frontal and temporal connectivity with brain volumetrics in CH-NATs and CH-PATs are reported in Supplementary Table 2.

Functional connectivity and HRV analysis

Spearman's correlation analysis was also conducted in both groups to explore the relationship between HRV metrics and EC during task-switching paradigms. In the task-switching condition, CH-PATs exhibited noteworthy findings, revealing significant negative correlations between frontal EC with Root mean square of the successive differences (RMSSD) ($r = -0.52$, $p = 0.020$). Conversely, CH-NATs demonstrated significant negative correlations between frontal connectivity and mean RR ($r = -0.87$, $p = 0.002$), as shown in Fig. 6. On the contrary, CH-NATs did not reveal significant correlations in RMSSD measures and brain connectivity as shown in Fig. 6.

Discussion

The main objective of the present biomarker study was to characterize the effects of the accumulation of $A\beta$ pathologies and tau concentrations on the

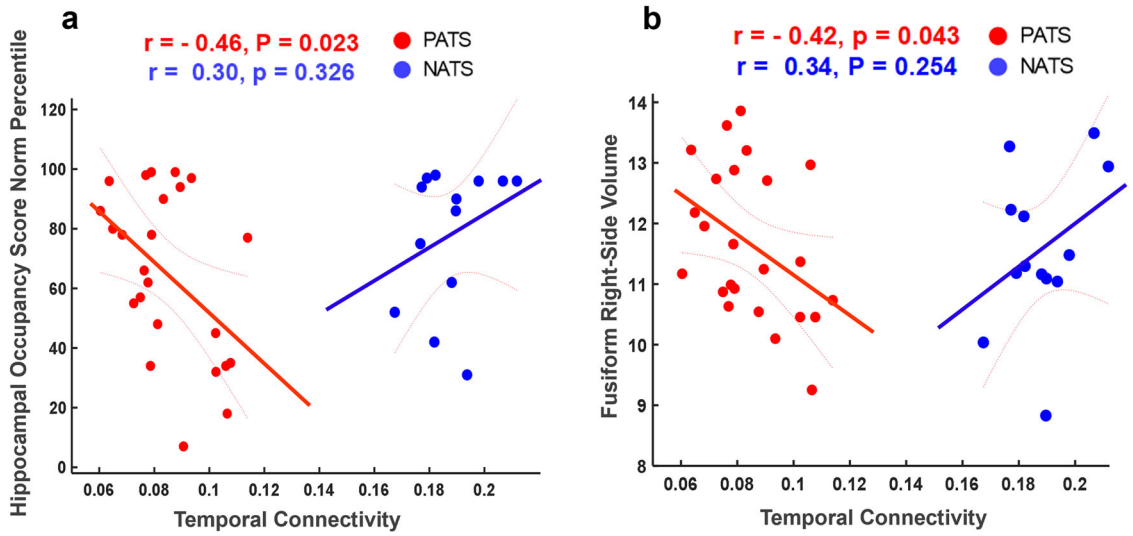

Fig. 5 | Correlation analysis between various brain volumetrics and directed functional connectivity in CH-PATs and CH-NATs. a A Correlation analysis between Hippocampal Occupancy Score (HOC) Norm Percentile and temporal EC in two groups;in two groups CH-NATs (blue scatter plots) and CH-PATs (red scatter plots). **b** Correlation between Fusiform Right Side Volume and temporal EC between two groups; CH-NATs and CH-PATs. A correlation analysis reveals the strength and direction of the association between brain volumetrics and brain connectivity. Spearman correlation was applied and the $p < 0.05$ and r (association directionality values) are shown.

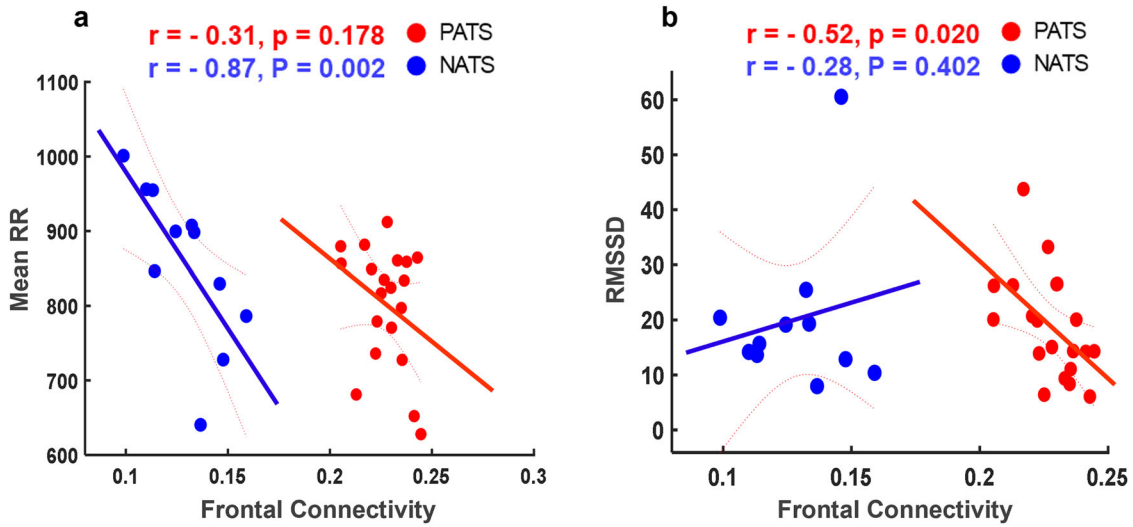

Fig. 6 | A correlation analysis between HRV measures and brain connectivity (frontal and temporal regions) in two groups CH-NATs (blue scatter plots) and CH-PATs (red scatter plots). a A correlation between mean RR and frontal EC during task switching for two groups CH-NATs and CH-PATs. **b** A correlation between resting RMSSD and frontal connectivity for the two groups. Spearman correlation was applied and p values were set to < 0.05 and r (association directionality values) are shown.

directed brain networks in CH individuals. Participants categorized into our CH-NAT and CH-PAT groups were asymptomatic, with normal neurocognitive tests, and were diagnosed based on CSF $A\beta42$ and Tau measures that were within the published ranges[6]. The CSF $A\beta42$/Tau ratio outperforms the CSF $A\beta42$ or tau levels individually to identify dementia and preclinical phases of AD. Abnormal amyloid levels and tau accumulation can disrupt synaptic function by interfering with neurotransmitter release and synaptic plasticity. This disruption can lead to neurotoxicity, microtubule destabilization, neuroinflammation, and alterations in the strength and efficiency of synaptic connections between neurons, ultimately affecting overall brain connectivity. In this exploratory study, we report on several important findings: (1) CH-PATs compared to CH-NATs, presented higher frontal EC, and lower temporal EC, independent from task difficulties. (2) CH-PATs presented significant correlations between temporal or frontal EC and other measures, including neuropsychological measurements (i.e., processing speed, executive functions, and working memory tests), MRI regional volumetrics, and HRV, supporting compensatory mechanisms. These changes are potentially linked to a less strategic approach while performing the task in CH-PATs, or no improvement in efficiency. These results may indicate that CH-PATs may present compensating mechanisms and may lack learning and self-improvement with functions that as seen in advanced intelligence for self-improving mode. Another similar example is during coding, using functions (temporal lobe in CH-NATs) can improve efficiency, while always using whole codes (frontal lobe) but limited functions (temporal lobe) can be exhaustive for CH-PATs.

The identification of effective EEG biomarkers associated with AD pathology holds substantial promise in unraveling the neural mechanisms underlying this neurodegenerative disorder and facilitating its early

diagnosis. Growing evidence suggests that EEG measurements reflect the capacity of AD neuropathology on brain neural signal transmission underlying cognitive processes[34–36]. However, the accuracy and reliability of different types of EEG biomarkers, i.e., power and entropy in facilitating the early detection and prediction of AD progression remain largely unknown. To our knowledge, this is the first study to evaluate the impact of promising EEG connectivity on detecting early AD pathology in CH individuals. We provide strong evidence supporting that the inclusion of multidimensional information (i.e., EEG biomarkers, CSF measures, brain volumetrics, and HRV) is highly effective in assessing patients' pre-symptomatic clinical status. Taken together, our findings suggest that brain connectivity has the potential for the early detection of risk for cognitive decline in CH individuals independently or in association with other measures. Notably, our study corroborates these findings and highlights the significance of EEG metrics and connectivity as pivotal biomarkers for revealing CH-PATs.

The Behavioral results of this study showed no significant differences between all CH-PATs and CH-NATs groups (results were reported previously in ref. 32). Additionally, the after-test survey suggested no subjective difficulty levels between the two groups. This indicates that, at the behavioral level, there is no evidence of cognitive decline in CH-PATs at this early stage of the disease. One possible explanation is that the cognitive deficits associated with CH-PATs are not yet severe enough to manifest at the behavioral level[37]. It is also possible that compensatory mechanisms and/or CR may contribute to similar behavioral performance in both groups[38]. When the brain switches attention between tasks, it successfully alternates, but consistent mental replacement of one task with another requires additional effort in terms of time and cognitive resources. This leads to switching costs, which we also observed in our study. Both CH-PATs and CH-NATs exhibited longer RTs during switch trials compared to repeat trials, indicating the presence of a successful switching cost effect[32,39,40]. Moreover, to investigate the possible contribution of task difficulty level to the EC differences, we selectively compared connectivity values between the best 50% performance of CH-PATs (Highest accuracy scores and lowest RT scores) and the lowest 50% performance from CH-NATs (lowest accuracy scores and highest RT scores) to bring down the potential differences and check if the frontal and temporal EC differences remained. Presumably, these subsets will bring CH-PATs and CH-NATs data closer in subjective difficulty/concentration. If connectivity analysis continues to exhibit consistent differences, it suggests that the connectivity patterns are fundamental, rather than solely results of task difficulty. Conversely, if the connectivity differences diminish, it indicates that they may indeed be influenced by subjective task difficulty. This approach was motivated by the desire to control for the influence of task difficulty on EC alterations and isolate the effects of intrinsic brain connectivity differences. By focusing on individuals with comparable task performance levels, we were able to minimize the confounding effects of task difficulty, ensuring that any observed EC differences were more likely attributable to inherent neurobiological factors rather than variations in task performance[41]. The good performance (increased ACC values and decreased RT values) in Fig. 3 may suggest that this group of CH-PATs did benefit from cognitive reserve, at least on neural activity during task switching. This also could be due to a compensatory increase in the number of neurons and/or synapses in CH-PATs.

During task switching processing compared to CH-NATs, CH-PATs exhibited higher alpha power values in the frontal region, while lower values were observed in temporal and parietal areas as shown in Fig. 1. These aberrations may signify two distinct pathophysiological alterations: the reduction in alpha power in AD pathology could be attributed to alterations in cortico-cortical connections[42]. We previously reported increased event-related resynchronization (ERD) in CH-PATs, compared to CH-NATs in the alpha band[32]. In contrast to ERD (Negative values calculated by wavelet transform and corrected with baseline), absolute alpha power (Positive values calculated by welch power) is a measure of the overall power that may detect changes in excitability alterations in the brain and does not provide specific information about task-related processing. ERD and absolute alpha power are both measures used in EEG analysis, but they capture different aspects of brain activity. Furthermore, evidentiary results have found higher resting-state alpha power manifestations in the frontal regions among MCI individuals compared to CH individuals[43]. This increase may suggest the recruitment of compensatory mechanisms. Individuals with a cognitive decline may show less vigilance to external stimuli in the resting state and may exhibit diminished capacity to recruit relevant brain regions when performing a task. Previous investigations have consistently reported slowing EEG activity among individuals with MCI and AD. For instance, a recent work substantiates the presence of distinct power resting state EEG rhythms in older individuals with subjective memory complaints (awareness of memory loss), notably showing greater theta power and a subtle reduction in EEG reactivity[44]. In addition, a decreased alpha/beta power and increased theta/delta power across various brain regions, including the frontal, temporal, parietal, and occipital areas[45] were reported. The degeneration of cholinergic neurons in the basal forebrain projecting to the hippocampus and neocortex is believed to play a pivotal role in this process[46]. The present study also examined the resting-state EEG power analysis in CH-PATs and CH-NATs. Our findings revealed no significant differences in EEG power between the two groups during the resting state. This lack of significant differences suggests that the EEG resting-state brain activity may not be significantly affected by the pathological amyloid/tau. Such results may indicate compensatory mechanisms or variability within the groups, which might contribute to the absence of significant differences. The absence of significance also may indicate that cognitive challenge can help in revealing subtle changes in brain activities[47,48].

In our investigation, we employed directed EC measures in the alpha frequency band, which are reliable, valid, and less influenced by confounding factors such as volume conduction[49]. Unlike undirected functional connectivity (i.e., coherence, phase lag index (PLI), and Phase Locked Value (PLV)) or Structural connectivity (anatomical links between neuronal populations), Effective connectivity (EC) (i.e., partial directed coherence (PDC)) among different EEG features examines the causal and directional influences between distant brain networks. Our study provides evidence of EEG changes associated with pre-clinical AD neuropathologies ($A\beta$ and tau). Specifically, we found a significant association between the $A\beta$ /tau in CSF and an increase in CH-PATs frontal alpha connectivity. Reduced levels of $A\beta$ peptides in the CSF indicate heightened $A\beta$ deposition in the brain, while elevated levels of CSF tau protein, derived from damaged neuronal microtubules, serve as reliable biological indicators of AD and predictors of MCI conversion[50]. It has been found that synaptic dysfunction is a fundamental deficit in AD, preceding the emergence of hallmark pathological changes[51]. Soluble $A\beta$ oligomers and tau fibrillar lesions disrupt synaptic plasticity and contribute to synaptic loss, resulting in the impairment of neural networks. Consequently, MCI and pre-symptomatic AD are better characterized as disruptions in functional and structural integration of neural systems rather than localized abnormalities. Our study observed increased frontal connectivity in CH-PATs. This finding suggests possible compensatory responses within executive networks and the presence of synaptotoxicity and neuronal dysfunction associated with presymptomatic AD-related pathology[52]. Furthermore, preclinical studies have suggested that increased synchrony in cortical circuits among individuals with pathological $A\beta$/tau may be attributed to reduced inhibitory neurotransmission mediated by GABAergic mechanisms rather than increased excitatory transmission[53]. Furthermore, tau was hypothesized to be associated with a breakdown in predictive neural coding[54].

We speculate that CH-NATs exhibited pronounced temporal lobe connectivity in terms of causal interactions, surpassing those observed in CH-PATs. These results align with existing evidence indicating that the preclinical stages and MCI are characterized by significant atrophy and hypometabolism primarily in the posterior hippocampal, cingulate, temporal, and parietal regions. Particularly, these affected regions collectively resemble the memory network and default mode network as delineated in healthy individuals using task-free fMRI paradigms[55]. In summary, decreased brain connectivity is believed to be associated with memory decline[56].

Furthermore, our analysis of EEG data using three distinct connectivity measures (that is, PDC, PLV, and wPLI) revealed complementary insights into neural connectivity patterns[57]. PDC analysis showed significant EC between the frontal and temporal cortices, pointing to greater information flow from these regions. In contrast, PLV identified significant phase synchronization between the frontal and occipital cortices, suggesting coupled activity potentially related to top-down visual attention processes[58]. WPLI results found significant phase synchronization in the frontal, parietal, and central cortices, indicating inhibitory effects of visuospatial attention, inhibition of return, and inhibitory control[59]. Different brain regions might be more involved in either directional influence or synchronization depending on the cognitive task. The synchronization (Measured by PLV and wPLI) between two regions could be due to a third region influencing both, or other indirect interactions. Conversely, PDC can be established without strong functional synchronization if the causal influence is strong enough to create a statistically significant correlation in their activities. The differences in how these methods handle noise, artifact, spatial, temporal resolutions, and the assumptions they create about neural dynamics can lead to variations in results. Notably, these three methods consistently identified the frontal cortex as a key hub of connectivity. These findings underscore the importance of the frontal cortex in the neural network and illustrate how different connectivity measures can provide a multifaceted understanding of brain activity[60].

Our results revealed significant associations between brain connectivity and performance on these neuropsychological measures. Regarding memory tasks (e.g., REY-O 3-MINUTE DELAY), CH-PATs show a strong positive correlation between frontal connectivity and performance on episodic memory tasks. This finding suggests that greater connectivity within the working memory brain networks is associated with greater efficiency[61]. Furthermore, we observed a significant negative correlation between frontal connectivity and executive functions tasks (that is, language animals tasks), indicating that decreased connectivity in the temporal or frontal regions is associated with poorer executive functions tasks and may indicate a neural compensatory mechanism. CH-PATs showed a positive correlation between frontal connectivity and Stroop color-naming task as compared to CH-NATs. This suggests that CH-PATs compensate for their processing speed decline by increasing their frontal cortex connectivity (specifically in regions linked with executive functions) to perform better on the Stroop color naming task. Moreover, we found many negative correlations between brain connectivity and attention tasks, indicating that greater connectivity in these regions is associated with decreased attentional performance[62]. These results underscore the importance of brain connectivity with memory and cognitive functioning[63]. The strong correlations observed between specific brain regions and performance on memory and cognitive tasks provide evidence for the role of neural networks in cognitive processes.

Furthermore, results suggest that the relationship between CR and parietal connectivity may vary across different patient populations, with the CH-NATs group showing a distinct pattern of negative correlation. Adults with higher levels of cognitive reserve (CR) are more likely to use other cognitive resources, such as memory strategies, to compensate for their memory impairments. Previous studies showed that individuals with a higher CR use additional brain regions associated with better memory task performance[64]. CR is assumed to reduce the risk of cognitive decline associated with brain changes related to aging by promoting the use of compensatory cognitive processes[65]. CR indicates the efficiency, capacity, and flexibility of cognitive processes in the presence of a challenge, which helps to explain the individual's ability to cope better with brain pathology (e.g., brain aging, delay of dementia symptoms, stroke) via more adaptable functional brain processes. Although actual biomarkers of CR are still questioned, a possible mechanism for CR has been hypothesized[66]. Neural reserve theory postulates that there exists an inter-individual variability in brain networks that function as a basis of any task. In CH-NATs, a higher CR was correlated with a lower parietal EC (more efficient), which was not observed in CH-PATs. This result may suggest that CR may be exhausted in CH-PATs during this task switching processing.

The association of MRI structural volumes and EEG brain connectivity in alpha may explain how neural structures and brain functions are coupled. The negative correlations in CH-PATs between temporal EC and these brain volumes suggest that a decrease in the volume of these brain regions may be associated with an increase in EC[67]. This could be due to a compensatory increase in the number of neurons and/or synapses in these brain regions. Previous studies have found that people with AD typically have smaller hippocampus than in HCs[68]. This suggests that the reduction of neurons in the hippocampus may constitute one of the initial alterations observed in AD[69]. Other brain regions that are often affected in AD include the temporal, the parietal, and the frontal lobes[69,70]. In late-onset AD, cortical atrophy initiates in the temporal cortex and subsequently extends to the parietal cortex via the cingulum bundle. In contrast, in early-onset AD, cortical atrophy originates in the parietal cortex and then spreads to the temporal cortex[71,72]. These regions are involved in a variety of cognitive functions, including language, memory, and executive function. Furthermore, recent research observed that both AD and MCI patients showed altered FC of the fusiform gyrus in a resting state compared to normal controls[73,74], which can help explain our findings in supplementary Table 2. As the disease progresses, the brain tissue in these regions may shrink, leading to further cognitive decline. Our findings uphold the notion that greater connectivity within the frontal regions is associated with brain compensation in pre-symptomatic AD[75]. This relationship aligns with previous studies highlighting the involvement of the frontal cortex in early AD pathology[10]. The results could provide evidence that enlarged regional volumes in CH-PATs may link with greater frontal EC and play a role in compensating for behavioral performance in the presence of AD pathologies.

Despite the probable clinical relevance of autonomic dysfunction in CH individuals with pathological *Aβ*/tau, only a few studies have evaluated HRV in presymptomatic AD. Our study observed a significant negative correlation between frontal connectivity and RMSSD in CH-PATs but not in CH-NATs. The level of brain connectivity may serve as a predictor of cognitive flexibility during a cognitive task, whereas HRV may specifically predict cognitive flexibility when influenced by neuronal oscillations[76]. The association of HRV, which measures autonomic function, and cardiovascular disease as well as cognitive dysfunction has been evidenced. There is a strong relationship between cardiovascular risk and an elevated likelihood of developing neurodegenerative diseases[77]. During the initial phases of AD, perturbations in the autonomic nervous system play a role in sustaining chronic hypoperfusion, thereby impacting the self-regulation of the brain and the functioning of the neurovascular unit. Conversely, neurodegenerative alterations characteristic of AD can exert an influence on autonomic functions and HRV by disrupting the vegetative networks situated in the insular cortex and brainstem[78]. This is in line with the previous findings that the preclinical dementia patients demonstrated parasympathetic regulation of slow waves is strongly associated with disrupted FC in the central nervous system[79]. Our data suggested that higher HRV (mean RR or RMSSD) is related to lower temporal and frontal connectivity in CH-NATs. CH-PATs also suggest that higher RMSSD is associated with decreased brain connectivity. Our study supports that memory and executive function networks are related to autonomic regulation and are affected by AD pathology.

The current study has several limitations. Firstly, the study's sample size was relatively modest, potentially limiting the generalizability of our findings to broader populations or distinct groups. Second, we used the 21-electrode EEG system to study brain connectivity (scalp potentials) in the brain cortex. Future research should focus on a high-density EEG system (i.e., 64, 128, or 256 electrodes) and compare the results with our findings. Third, a notable limitation of this study is the time difference in data collection, with MRI and EEG data being acquired at different time points. This misalignment could potentially introduce confounding variables related to

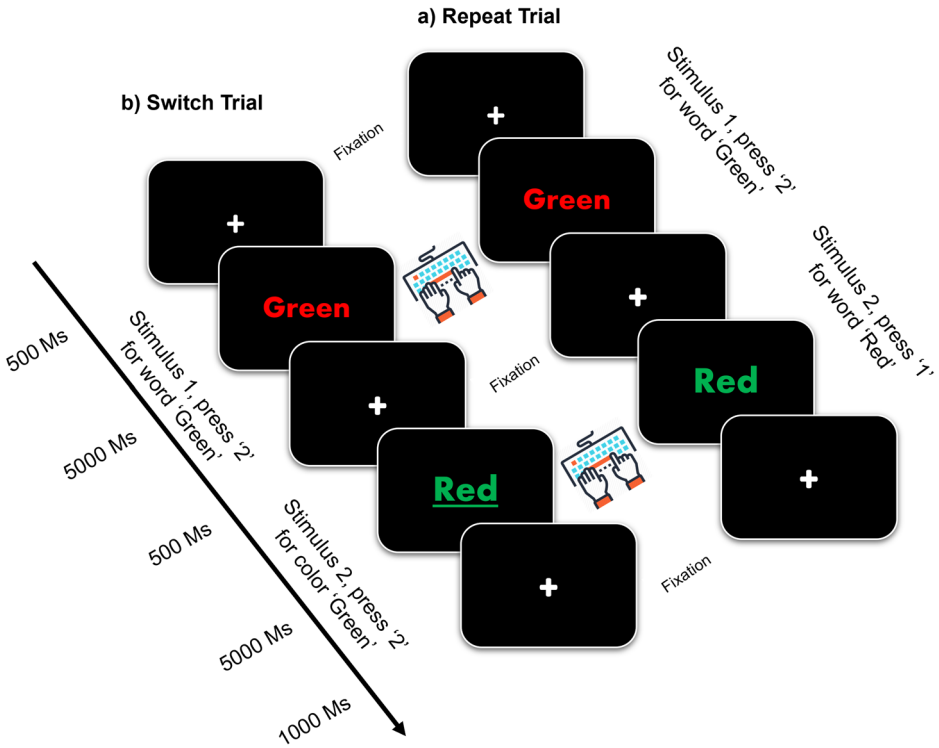

Fig. 7 | Task switching testing paradigms. Each trial includes two sequential stimuli. Each stimulus is incongruent colored word. Participants were requested to respond to the word itself (no-underline), or to the color of the ink (underlined), by pressing a button ("1" for red, "2" for green). Tasks include a random mixture of low-load repeat trials (**a**) or high-load switch trials (**b**). The paradigm is described from our previous work[32].

alterations in the participants' electrophysiological states or external environmental factors over time. Fourth, our analysis was performed at the sensor-space level rather than at the source-space level. While sensor-level analysis offers valuable insights into neural activity patterns, it lacks the precision and specificity that source-level analysis can provide in localizing the origins of these signals within the brain. Fifth, we considered CSF *Aβ* and tau in classifying our cohorts. Future research endeavors may explore brain connectivity using PET or plasma *Aβ* and tau to study pre-clinical AD progression. Lastly, a significant limitation in estimating causal information flow among brain regions, such as with PDC, particularly with multichannel non-invasive recordings, is the influence of volume conduction arising from surrounding active neuronal sources. Future investigations should explore alternative connectivity algorithms less sensitive to volume conduction and validate findings using high-temporal-resolution methodologies such as MRI or DTI.

To conclude, AD pathology manifests several years before clinical symptoms are recognized, termed the preclinical stage. We investigated this stage to assess whether brain connectivity could detect this early pathophysiology. The results of this study showed the potential of EC as a non-invasive tool in isolating the asymptomatic participants with normal CSF biomarker (CH-NATs)levels from asymptomatic participants with AD (CH-PATs) during task switching. Reduced temporal EC and increased frontal EC were reported in CH-PATs compared to CH-NATs, independent of task difficulties. The increased frontal EC and/or decreased temporal EC in CH-PATs are linked with disrupted brain volumes, neuropsychological, HRV, and CR, suggesting a compensatory mechanism in the presence of AD pathology to retain the same behavioral performance. Our findings indicate that *Aβ*/tau pathology may affect specific EEG networks with systemic structural/functional compensations. Overall, EC is a useful, non-invasive tool for assessing EEG-functional-network activities and provides a better understanding of the neurophysiological mechanisms underlying Alzheimer's disease.

Methods

Participants

Forty-six cognitively healthy elderly participants were recruited locally through local newspapers and newsletters, the Pasadena Huntington Hospital Senior Health Network, and visits to the senior centers. All participants consented via an Institutional Review Board (IRB) approved protocol (HMRI # 33797). Assessments included collecting demographic data, physical exams, fasting blood studies, disease severity and disability scales, and CSF *Aβ*/tau measurements[6]. Inclusion criteria: over 60 years, classified as CH after a comprehensive neuropsychological battery, as referenced in detail[6]. Exclusion criteria: other active, untreated disease, use of anticoagulants, or other contraindications to lumbar puncture.

CSF Amyloid/tau analysis

We reported a cutoff ratio of *Aβ*42/total tau (2.7132) provided at least 85% sensitivity in discriminating AD from non-AD participants; we then used this regression to assign CH participants (CH) into 2 groups, one with normal CSF *Aβ*/total tau (CH-NATs) and the other with pathological *Aβ*/total tau (CH-PATs). As provisional evidence for the capacity of this CSF *Aβ*/total tau to predict clinical decline, a longitudinal study found that 40% of CH-PATs declined cognitively over 4 years to MCI, or AD, while none of the CH-NATs declined[39,40]. A detailed description of the data collection, methodological aspects of the entire process, and CSF data analysis procedures have been documented in our prior studies[6,32,39].

Task switching paradigms

During the resting state baseline, participants were instructed to remain still and relax for 5 min with their eyes open, followed by another 5 min with their eyes closed. For the task-switching testing each trial consisted of two sequential stimuli, both presenting incongruent colored words (e.g., the word 'Red' in green color or the word 'Green' in red color), with or without an underline (see Fig. 7). Participants were instructed to press a button labeled '1' for red and '2' for green, indicating either the color (c) when underlined or the word (w) when not underlined. The trials were categorized into low-load repeat (color-color (cC) or word-word (wW)) or high-load switching (cW or wC) trials, with the second stimulus denoted using superscript to indicate the study target. The task-switching phase was comprised of three mixed blocks, each containing 64 trials. The blocks included all four conditions (cC, wW, cW, wC) in a random sequence with equal weightage. Our analysis focused on the cW task due to the presence of the persisting task-set inhibition[80].

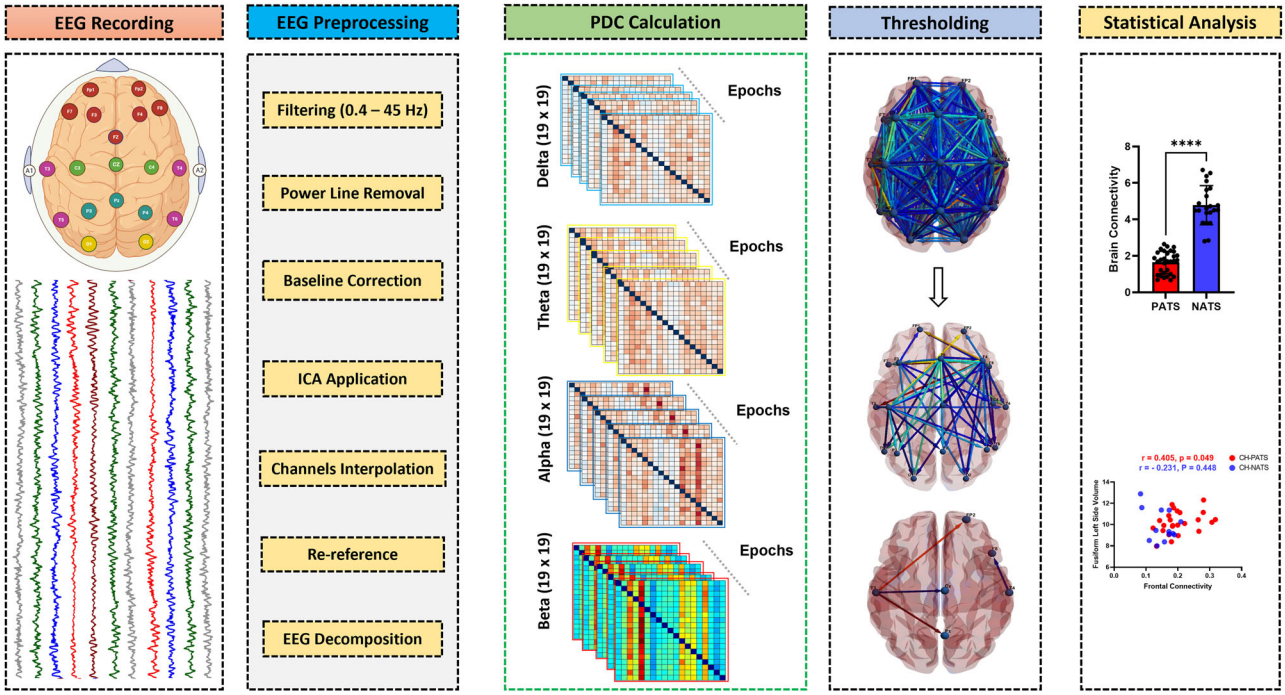

Fig. 8 | Schematic representation of the main steps involved in EEG data processing. From raw EEG signals, cortical activity is achieved by means of high-resolution EEG techniques. It shows the HAPPE pipeline's pre-processing steps including ICA, the estimation of directed FC from the cortical time series, threshold application, and eventually the statistical analysis. The Schematic figure also shows the proportional threshold on the PDC metrics by maintaining a proportion p ($0 < p < 1$) of the high dense connections and setting these connections to the same connectivity value, with all other connections set to 0[86]. The selection of the optimum thresholding value was based on global cost efficiency[96]. The brain network statistics are performed by *t*-test and Spearman's rank correlation coefficient or Pearson correlation coefficients where appropriate.

EEG data acquisition and processing

All EEG data were collected during the resting state (eyes closed) or during the switching-task challenge[32]. A 21-head-sensor, dry electrode system (Quasar Wearable Sensing, DSI-24, San Diego, CA, USA) was used to collect EEG signals. Sensor configuration followed the international 10–20 system. EEG signals were sampled at 300 Hz, and bandpass filtered between 0.4 and 45 Hz. For artifact rejection, we applied a − 100 to 100 μV voltage threshold to detect bad epochs. In short, the visual inspection of epochs was performed based on a minimum of artifacts (e.g., excessive muscle activity, eye blinks) and drowsiness. In our study, drowsiness was inspected in EEG signals through careful visual inspection. Specifically, trained individuals examined EEG recordings for characteristic patterns associated with drowsiness, such as slowing of brainwave frequencies, increased theta activity, or intermittent bursts of alpha waves. Inspecting drowsiness is crucial to keep participants awake and alert (verbal notification) to ensure data quality, participant safety, and the validity of our experimental findings in our recordings. When an adequate level of quality was not obtained, we either substituted the epochs with alternative ones or eliminated the EEG data from further analysis if there were no sufficient epochs from the same subject available for analysis. Data quality refers to the standard of quality considered acceptable for the EEG data to be considered reliable for further analysis. This standard encompasses different factors including signal clarity, absence of artifacts, and adherence to predefined criteria for data integrity. For better signal processing, electrooculographic, electrocardiographic, and electromyography were recorded by 3 auxiliary sensors. A trigger channel encoded the time of color-word stimuli onset, the participants' responses, and the type of test (C or W) for further analysis.

The continuous baseline EEG data were initially converted from the DSI-24 format to MATLAB format (R2022a)[38]. To ensure data quality and remove artifacts, a preprocessing pipeline designed explicitly for developmental EEG data, known as the Harvard Automated Processing Pipeline for EEG (HAPPE), was employed[38]. This subset consisted of 21 channels; Frontal (Fp1, Fp2, F7, F3, Fz, F4, F8), Temporal (T3, T4, T5, T6), Parietal (P3, PZ, P4), Occipital (O1, O2), Central (C3, CZ, C4), and mastoidal (A1, A2), as shown in Fig. 8. The EEG signals were then referenced to the two mastoids/earlobes electrodes A1 and A2. Before independent component analysis (ICA), a 0.4 Hz digital high-pass filter, and a 45 Hz low-pass filter were applied to the EEG data to remove non-stationary signal drifts across the recording. HAPPE's artifact removal steps encompassed the elimination of 60 Hz electrical noise using CleanLine's multi-taper approach, rejection of bad channels, and removal of participant-related artifacts (e.g., eye blinks, movement, muscle activity) through ICA with automated component rejection via EEGLAB and the Multiple Artifact Rejection Algorithm (MARA)[81]. After artifact rejection, any channels removed during bad channel rejection were reconstructed using spherical interpolation to mitigate spatial bias in re-referencing. The resting-state EEG data were segmented into contiguous 2-s windows, and segments containing retained artifacts were rejected based on HAPPE's amplitude and joint probability criteria, consistent with prior research on developmental EEG[82]. Importantly, there were no significant differences between outcome groups in terms of the mean lengths of the processed EEG data or any of the HAPPE data quality measures. Significant features were determined ($p < 0.05$), and assessed for the between groups using Student's *t*-test)[82].

A Fast Fourier Transform (FFT) with multitaper windowing was used to decompose the EEG signal into power for each 2-s segment for each of the channels of interest. For each of the four frequency bands, the summed power across all frequencies within the band was calculated as the measure of total power in that frequency band. All segmentation parameters and analysis windows are consistent with connectivity metrics and FFT was conducted using a Hanning window. Each participant's data was averaged across the epochs for each electrode and the mean alpha power was computed for each of the following frequency bands: delta (0.4–4 Hz), theta (4–8 Hz), alpha (8–12 Hz), and beta (12–30 Hz). We selected a time window from 200 ms to 550 ms after stimulus onset as it detects brain responses associated with diverse cognitive functions, such as attention, working memory, decision-making, integration of incoming words, and emotion processing[83]. The data analysis process is illustrated in the block diagram in Fig. 8.

Brain connectivity networks and information flow

Partial directed coherence (PDC) is one measure of the Granger causality which provides insights about the directionality of information between the brain nodes. PDC is based on the consideration that knowledge of the "driver's" past increases the prediction of the "receiver's" present state, compared to only using the receiver's past. In the presence of volume conduction, however, all EEG channels mutually "drive" each other in this respect. PDC is derived from coefficients of a multivariate autoregressive (MVAR) model, which additionally depends on the scaling of the data. Interestingly, this scaling dependency is sufficient to yield significant spurious information flow from low-variance to high-variance temporally and spatially white noise channels. The MVAR uses Akaike information criterion (AIC) and Schwarz information to select the model order of MVAR[84,85]. In this study, the average MVAR model order p for all subjects was 7. Models with lower AIC are principally preferred. PDC is a frequency-domain approach to denote the direct linear relationship between two different signals $y_i(t)$ and $y_j(t)$ (equation 1) once remarked jointly with a set of other signals. Considering $Y(t)$ the set of all observed time series, it can be depicted as an autoregressive model as follows: where p represents the model order, $\boldsymbol{\varepsilon}$(t) is the prediction error matrix and A_k are the coefficients matrix with a_{ij} elements in which denotes the relation between signals at lag k. $\boldsymbol{\varepsilon}$(t) has a covariance matrix ξ and their coefficients are usually a white noise with zero mean. This results in PDC factor (π_{ij}) and partial coherence function ($|k_{ij}[f]|^2$) that indicates the strength and the direction of communication at frequency f.

Therefore, the PDC value from channel j to channel i can be expressed as follows:

$$\pi_{ij}[f] = \frac{\bar{A}_{ij}(f)}{\sqrt{{}_j - H(\mathrm{f})^{\xi^{-1}}\ \bar{a}_j(f)}} \tag{1}$$

$$k_{ij}[f] = \pi_i^H(\mathrm{f})^{\xi^{-1}}\ \pi_j(f) \tag{2}$$

where, $(\bar{a}_i)(f)(i = 1, 2, \ldots M)$ represents the i^{th} column of the matrix $\bar{A}(f)$ and π_{ij} represents the strength of causal interaction of the information flow from channel j to channel i at a frequency of f.

$H[f]$ is the Hermitian matrix which is equal to $\bar{A}^{-1}[f]$. $\bar{A}_{ij}(f)$ is the complement of $A_{ij}(f)$ and represents the transfer function from $y_j[t]$ to $y_i[t]$ being also an element of $A[f]$ matrix. Finally, $a_j[f]$ is the j^{th} column of $A[f]$ and π_i is the i^{th} row of π_{ij}.

We applied the proportional threshold on the PDC metrics by maintaining a proportion p $(0 < p < 1)$ of the highly dense connections and setting these connections to the same connectivity value, with all other connections set to 0[86]. The selection of the optimum threshold value was based on global cost efficiency. Proportional thresholding is a commonly used analysis step in reconstructing functional brain networks to ensure equal density across patient and control samples. The proportional threshold method is employed to highlight the most robust and significant connections while reducing visual clutter caused by weaker or less relevant connections. The MVAR model is a mathematical model commonly used in time series analysis to describe the relationship between an observation and a linear combination of its past observations. This MVAR model is generated using the two-time series for a specific frequency f, A_k is the MVAR model in the discrete domain, is the covariance of the cross-spectral density matrix, k is the number of EEG channels, and I is the identity matrix. Calculation of the PDC values leads to a large matrix that describes the connectivity between the EEG channels, as shown in equation (1), where $ij(f)$ is the individual PDC value calculated from the time series i to j at frequency f. The PDC values range between 0 and 1 depending on how well one time series predicts the other. The strength of a measure such as PDC is apparent in its formulation because it is normalized according to the destination. When analyzing time series, this operation is taken in a short time Fourier transform approach. A 50 percent overlap between windows, with a window length of 400 Ms, is chosen to capture events that may fall on the border between windows. To reduce memory requirements, frequencies are divided into evenly spaced bins, typically a power of 2; here we chose 30. For k channels, there will be a k x k x 30 x t matrix of PDC values. The first dimension is the source channel and the second corresponds to the destination.

Brain phase synchronization

Phase synchronization analysis is crucial in understanding undirected functional connectivity in brain networks derived from EEG data. The Phase Lag Index (PLI) is a widely used measure in neuroscience that quantifies the consistency of phase differences between neural oscillations across different brain regions. Nonetheless, the Weighted Phase Lag Index (wPLI) extends the PLI by considering the magnitudes of the phase differences. This enhancement accounts for the strength of phase coupling between neural oscillations in addition to their consistency. The wPLI is a robust functional connectivity approach used in EEG connectivity analysis, because of its high insensitivity to common sources and volume conduction effects. The formula for wPLI is given by:

$$wPLI = \frac{|\langle \sin(\Delta\phi(t)) \rangle|}{\langle |\sin(\Delta\phi(t))| \rangle} \tag{3}$$

Where, $|\Delta\phi(t)|$ represents the magnitude of the phase difference. wPLI provides a more refined measure of functional connectivity, capturing both the consistency and strength of phase coupling between brain regions. In contrast to PLI, the wPLI adjusts the weighting of the cross-spectrum based on the magnitude of its imaginary component. It eliminates the influence of cross-spectrum elements (phase lacking) near the real axis (0, π, or 2π), which are susceptible to small noise perturbations that might alter their true sign due to the volume conduction effects.

Moreover, the phase locking value (PLV) method is commonly used for calculating the correlation between two electrodes. The PLV is a statistic that can be used to investigate EEG data for task-induced changes in the long-range synchronization of neural activity. To calculate the PLV, two time series are first spectrally decomposed at a given frequency, f_0, to obtain an instantaneous phase estimate at each time point. Phase synchronization between two narrow-band signals is frequently characterized by the PLV. Consider a pair of real signals $s_1(t)$ and $s_2(t)$, that have been band-pass filtered to a frequency range of interest. Analytic signals $z_i(t) = A_i(t)e^{j\phi_i(t)}$ for $i = \{1, 2\}$ and $j = \sqrt{-1}$ are obtained from $s_i(t)$ using the Hilbert transform:

$$z_i(t) = s_i(t) + jHT(s_i(t)) \tag{4}$$

where $HT(s_i(t))$ is the Hilbert transform of $s_i(t)$ defined as:

$$HT(s_i(t)) = \frac{1}{\pi} P.V. \int_{-\infty}^{\infty} \frac{s_i(t)}{t - \tau} d\tau \tag{5}$$

and $P.V.$ denotes the Cauchy principal value. Once the analytic signals are defined, the relative phase can be computed as:

$$\Delta\phi(t) = \arg\left(\frac{z_1(t)z_2^*(t)}{|z_1(t)||z_2(t)|}\right) \tag{6}$$

The instantaneous PLV is then defined as[87]:

$$PLV(t) =: |E[e^{j\Delta\phi(t)}]| \tag{7}$$

where $E[.]$ denotes the expected value. The PLV takes values on [0, 1] with 0 reflecting the case where there is no phase synchrony and 1 where the relative phase between the two signals is identical in all trials. PLV can therefore be viewed as a measure of trial-to-trial variability in the relative phases of two signals. In this work, we use the Hilbert transform, but the continuous Morlet wavelet transform can also be used to compute complex signals, producing separate band-pass signals for each scaling of the wavelet[88]. The connectivity results associated with wPLI and PLV are presented in the supplemental section (Figs. S1 and S2).

Neuropsychological tests and cognitive reserve

Several tests of working memory, language, executive function, and processing speed were considered in our analysis. A full description of these tests and their references were reported in these studies[6,89].

One crucial factor that has not been taken into account in the previously described studies on strategy use is the potential role of Cognitive reserve (CR) (brain's ability to withstand aging or pathology by employing compensatory mechanisms)[90]. CR indicates the effectiveness, capability, and adaptability of cognitive processes during cognitive challenges or pathology. This phenomenon elucidates an individual's capacity to manage brain-related issues such as aging, and delayed onset of dementia symptoms. Various proxies are used to measure CR, including educational level, verbal intelligence quotient (IQ), engagement in work, social interactions, and/or participation in leisure activities[91]. Presently, composite measures offer the most comprehensive assessment of CR, such as education, occupational complexity, and leisure activities. In our study, both IQ estimation and education level were used as proxies for CR. First, scores were transformed into Z-scores. Subsequently, the education and IQ Z-scores were averaged into a single cognitive reserve (CR) score[64,66,92].

Structural MRI data acquisition

All MRI images were acquired at the Advanced Imaging and Spectroscopy Center of the Huntington Medical Research Institutes (Pasadena, CA) using a 1.5 Tesla General Electric (GE) clinical scanner with an 8-channel high-resolution head coil. A brief description of MRI and NeuroQuant (Cortechs Labs.ai Inc, San Diego, CA, USA) analyses was reported in our published work[93]. Several brain regions were selected to examine the correlation between brain connectivity and brain atrophy in CH-NATs and CH-PATs. These regions include the fusiform cortex, frontal cortex, hippocampus, entorhinal Cortex, and Amygdala. The normalization factors are often based on automated intracranial volume (ICV) measurements or scaling factors from skull-based or whole-head-based registration to a standard template[94,95].

ECG and HRV analysis

We examined the correlation between EC and HRV measures. Raw electrocardiogram (ECG) data were collected during the task-switching using AcqKnowledge software (BIOPAC Systems, Inc., Goleta, CA). ECG and HRV recording and analysis details were reported in our previous work[32]. A correlation between CH-PATS and CH-NATs was conducted between brain connectivity and HRV time domain measures (i.e., NN intervals (RR), heart rate (HR), standard deviation of NN (SDNN), and root mean squared successive differences (RMSSD)) and frequency domain (i.e., low frequency (LF) and high-frequency (HF)).

Statistics and reproducibility

We employed a parametric two-sample t-test, using Bonferroni–Holm correction method, to assess the connection metrics between CH-NATs and CH-PATs. Before conducting the statistical analysis, we used the Kolmogorov-Smirnov method to test the normal distribution of the data. A p-value ($p < 0.05$) was used to identify the significant differences between CH-NATs and CH-PATs at the group level. All data are presented as (mean ± SD). Finally, Spearman's or Pearson correlation was applied to study the association between brain connectivity and neuropsychological, CR scores, brain volumetric, and HRV scores. The $p < 0.05$ and r (association directionality values) are shown.

All statistical analyses were performed using GraphPad prism statistics software (version 9.5.0) and R programming language (version 2023.06.0), and Matlab (version 2022A, The Mathworks, Inc).

Reporting summary

Further information on research design is available in the Nature Portfolio Reporting Summary linked to this article.

Data availability

Raw data were generated at Huntington Medical Research Institutes (HMRI). All data generated or analyzed during this study are included in this published article and its supplementary information files, specifically in Supplementary Data 1. Derived data and Matlab codes supporting the findings of this study are available from the corresponding author AA on valid request.

Received: 16 January 2024; Accepted: 1 August 2024;
Published online: 23 August 2024

References

1. Nicaise, S. et al. Alzheimer and the Mediterranean report 2016: overview–challenges–perspectives (Monegasque Association for Research on Alzheimer's disease (AMPA), 2016).
2. Prince, M. et al. *World Alzheimer Report 2015. The Global Impact of Dementia: An analysis of prevalence, incidence, cost and trends*. Ph.D. thesis, Alzheimer's Disease International (2015).
3. Chehrehnegar, N. et al. Early detection of cognitive disturbances in mild cognitive impairment: a systematic review of observational studies. *Psychogeriatrics* **20**, 212–228 (2020).
4. Sharma, L. et al. Promising protein biomarkers in the early diagnosis of Alzheimer's disease. *Metab. Brain Dis.* **37**, 1727–1744 (2022).
5. Leyhe, T., Müller, S., Milian, M., Eschweiler, G. W. & Saur, R. Impairment of episodic and semantic autobiographical memory in patients with mild cognitive impairment and early Alzheimer's disease. *Neuropsychologia* **47**, 2464–2469 (2009).
6. Harrington, M. G. et al. Executive function changes before memory in preclinical Alzheimer's pathology: a prospective, cross-sectional, case control study. *PloS One* **8**, e79378 (2013).
7. Allain, P., Etcharry-Bouyx, F. & Verny, C. Executive functions in clinical and preclinical Alzheimer's disease. *Rev. Neurol.* **169**, 695–708 (2013).
8. Aluise, C. D. et al. Redox proteomics analysis of brains from subjects with amnestic mild cognitive impairment compared to brains from subjects with preclinical Alzheimer's disease: insights into memory loss in mci. *J. Alzheimer's. Dis.* **23**, 257–269 (2011).
9. Guan, Z.-Z., Zhang, X., Ravid, R. & Nordberg, A. Decreased protein levels of nicotinic receptor subunits in the hippocampus and temporal cortex of patients with Alzheimer's disease. *J. Neurochem.* **74**, 237–243 (2000).
10. Kashani, A. et al. Loss of vglut1 and vglut2 in the prefrontal cortex is correlated with cognitive decline in Alzheimer disease. *Neurobiol. Aging* **29**, 1619–1630 (2008).
11. Amieva, H. et al. Evidencing inhibitory deficits in Alzheimer's disease through interference effects and shifting disabilities in the Stroop test. *Arch. Clin. Neuropsychol.* **19**, 791–803 (2004).
12. Belleville, S., Chertkow, H. & Gauthier, S. Working memory and control of attention in persons with Alzheimer's disease and mild cognitive impairment. *Neuropsychology* **21**, 458 (2007).
13. Wang, Q. et al. Risk assessment and stratification of mild cognitive impairment among the Chinese elderly: attention to modifiable risk factors. *J. Epidemiol. Community Health* (2023).
14. Lee, D., Park, J. Y. & Kim, W. J. Altered functional connectivity of the default mode and dorsal attention network in subjective cognitive decline. *J. Psychiatr. Res.* **159**, 165–171 (2023).
15. Villemagne, V. L. et al. Amyloid β deposition, neurodegeneration, and cognitive decline in sporadic Alzheimer's disease: a prospective cohort study. *Lancet Neurol.* **12**, 357–367 (2013).
16. Park, J.-C. et al. Plasma tau/amyloid-β1–42 ratio predicts brain tau deposition and neurodegeneration in Alzheimer's disease. *Brain* **142**, 771–786 (2019).
17. Kwak, S. S. et al. Amyloid-β42/40 ratio drives tau pathology in 3d human neural cell culture models of Alzheimer's disease. *Nat. Commun.* **11**, 1377 (2020).
18. Wang, L. et al. Cerebrospinal fluid proteins predict longitudinal hippocampal degeneration in early-stage dementia of the Alzheimer type. *Alzheimer Dis. Assoc. Disord.* **26**, 314–321 (2012).

19. Fagan, A. M. et al. Comparison of analytical platforms for cerebrospinal fluid measures of β-amyloid 1-42, total tau, and p-tau181 for identifying Alzheimer disease amyloid plaque pathology. *Arch. Neurol.* **68**, 1137–1144 (2011).
20. Pichet Binette, A. et al. Amyloid-associated increases in soluble tau relate to tau aggregation rates and cognitive decline in early Alzheimer's disease. *Nat. Commun.* **13**, 6635 (2022).
21. Rodriguez-Vieitez, E. et al. Association of cortical microstructure with amyloid-β and tau: impact on cognitive decline, neurodegeneration, and clinical progression in older adults. *Mol. Psychiatry* **26**, 7813–7822 (2021).
22. Hoops, S. et al. Validity of the MoCA and MMSE in the detection of MCI and dementia in Parkinson disease. *Neurology* **73**, 1738–1745 (2009).
23. Matsuoka, T., Imai, A. & Narumoto, J. Neuroimaging of mild behavioral impairment: a systematic review. *Psychiatry Clin. Neurosci. Rep.* **2**, e81 (2023).
24. Nicolini, P. et al. Autonomic function predicts cognitive decline in mild cognitive impairment: Evidence from power spectral analysis of heart rate variability in a longitudinal study. *Front. Aging Neurosci.* **14**, 886023 (2022).
25. Ebinger, J. E. et al. Blood pressure variability supersedes heart rate variability as a real-world measure of dementia risk. *Sci. Rep.* **14**, 1838 (2024).
26. Molloy, C. et al. Resting heart rate (variability) and cognition relationships reveal cognitively healthy individuals with pathological amyloid/tau ratio. *Front. Epidemiol.* **3**, 1168847 (2023).
27. Palmqvist, S. et al. Earliest accumulation of β-amyloid occurs within the default-mode network and concurrently affects brain connectivity. *Nat. Commun.* **8**, 1214 (2017).
28. Yu, M., Sporns, O. & Saykin, A. J. The human connectome in Alzheimer disease—relationship to biomarkers and genetics. *Nat. Rev. Neurol.* **17**, 545–563 (2021).
29. Moretti, D. V. Understanding early dementia: Eeg, MRI, spect and memory evaluation. *Transl. Neurosci.* **6**, 32–46 (2015).
30. Kim, N. H. et al. Pet-validated eeg-machine learning algorithm predicts brain amyloid pathology in pre-dementia Alzheimer's disease. *Alzheimer's. Dement.* **19**, e064436 (2023).
31. Canuet, L. et al. Network disruption and cerebrospinal fluid amyloid-beta and phospho-tau levels in mild cognitive impairment. *J. Neurosci.* **35**, 10325–10330 (2015).
32. Arechavala, R. J. et al. Task switching reveals abnormal brain-heart electrophysiological signatures in cognitively healthy individuals with abnormal csf amyloid/tau, a pilot study. *Int. J. Psychophysiol.* **170**, 102–111 (2021).
33. Huang, S.-Y. et al. Characteristic patterns of inter-and intra-hemispheric metabolic connectivity in patients with stable and progressive mild cognitive impairment and Alzheimer's disease. *Sci. Rep.* **8**, 13807 (2018).
34. Vecchio, F. et al. Sustainable method for Alzheimer dementia prediction in mild cognitive impairment: Electroencephalographic connectivity and graph theory combined with apolipoprotein e. *Ann. Neurol.* **84**, 302–314 (2018).
35. Moretti, D. et al. Specific eeg changes associated with atrophy of hippocampus in subjects with mild cognitive impairment and Alzheimer's disease. *Int. J. Alzheimer's Dis.* **2012**, 253153 (2012).
36. McBride, J. C. et al. Spectral and complexity analysis of scalp EEG characteristics for mild cognitive impairment and early Alzheimer's disease. *Comput. Methods Prog. Biomed.* **114**, 153–163 (2014).
37. Trinh, T.-T. et al. Identifying individuals with mild cognitive impairment using working memory-induced intra-subject variability of resting-state eegs. *Front. Comput. Neurosci.* **15**, 700467 (2021).
38. Gabard-Durnam, L. J., Mendez Leal, A. S., Wilkinson, C. L. & Levin, A. R. The Harvard automated processing pipeline for electroencephalography (happe): standardized processing software for developmental and high-artifact data. *Front. Neurosci.* **12**, 97 (2018).
39. Arakaki, X. et al. Alpha desynchronization/synchronization during working memory testing is compromised in acute mild traumatic brain injury (mtbi). *PloS One* **13**, e0188101 (2018).
40. Arakaki, X. et al. A study of alpha desynchronization, heart rate, and mri during Stroop testing unmasks pre-symptomatic Alzheimer's disease: Eeg biomarkers of Alzheimer's disease in pre-symptomatic and symptomatic patients: Multimodal validation from international projects. *Alzheimer Dement.* **16**, e042793 (2020).
41. Philiastides, M. G., Ratcliff, R. & Sajda, P. Neural representation of task difficulty and decision making during perceptual categorization: a timing diagram. *J. Neurosci.* **26**, 8965–8975 (2006).
42. Wang, R. et al. Power spectral density and coherence analysis of Alzheimer's eeg. *Cogn. Neurodyn.* **9**, 291–304 (2015).
43. Gaubert, S. et al. Eeg evidence of compensatory mechanisms in preclinical Alzheimer's disease. *Brain* **142**, 2096–2112 (2019).
44. Perez, V. et al. Eeg markers and subjective memory complaints in young and older people. *Int. J. Psychophysiol.* **182**, 23–31 (2022).
45. Jiao, B. et al. Neural biomarker diagnosis and prediction to mild cognitive impairment and Alzheimer's disease using eeg technology. *Alzheimer's. Res. Ther.* **15**, 1–14 (2023).
46. Fahnestock, M. & Shekari, A. Prongf and neurodegeneration in Alzheimer's disease. *Front. Neurosci.* **13**, 440994 (2019).
47. Hearne, L. J. et al. Increased cognitive complexity reveals abnormal brain network activity in individuals with corpus callosum dysgenesis. *NeuroImage: Clin.* **21**, 101595 (2019).
48. Jeong, H. T., Youn, Y. C., Sung, H.-H. & Kim, S. Y. Power spectral changes of quantitative eeg in the subjective cognitive decline: comparison of community normal control groups. *Neuropsychiatr. Dis. Treat.* **21**, 2783–2790 (2021).
49. Briels, C. T. et al. Reproducibility of EEG functional connectivity in Alzheimer's disease. *Alzheimer's. Res. Ther.* **12**, 1–14 (2020).
50. Vlassenko, A. G., Benzinger, T. L. & Morris, J. C. Pet amyloid-beta imaging in preclinical Alzheimer's disease. *Biochim. Biophys. Acta (BBA)-Mol. Basis Dis.* **1822**, 370–379 (2012).
51. Grandjean, J. et al. Early alterations in functional connectivity and white matter structure in a transgenic mouse model of cerebral amyloidosis. *J. Neurosci.* **34**, 13780–13789 (2014).
52. Canuet, L. et al. Resting-state network disruption and *APOE* genotype in Alzheimer's disease: a *lagged* functional connectivity study *PLoS ONE*, **7**, e46289. https://doi.org/10.1371/journal.pone.0046289 (2012).
53. Palop, J. J. & Mucke, L. Amyloid-β–induced neuronal dysfunction in Alzheimer's disease: from synapses toward neural networks. *Nat. Neurosci.* **13**, 812–818 (2010).
54. Mohanta, S. et al. Receptors, circuits and neural dynamics for prediction. *Available at SSRN 3659396* (2021).
55. Greicius, M. D., Krasnow, B., Reiss, A. L. & Menon, V. Functional connectivity in the resting brain: a network analysis of the default mode hypothesis. *Proc. Natl. Acad. Sci. USA* **100**, 253–258 (2003).
56. Farràs-Permanyer, L., Guàrdia-Olmos, J. & Peró-Cebollero, M. Mild cognitive impairment and f MRI studies of brain functional connectivity: the state of the art. *Front. Psychol.* **6**, 1095 (2015).
57. Babiloni, F. et al. Hypermethods for eeg hyperscanning. In *2006 International Conference of the IEEE Engineering in Medicine and Biology Society*, 3666–3669 (IEEE, 2006).
58. Gilbert, C. D. & Li, W. Top-down influences on visual processing. *Nat. Rev. Neurosci.* **14**, 350–363 (2013).
59. Fernández, P. J., Vivas, A. B., Chechlacz, M. & Fuentes, L. J. The role of the parietal cortex in inhibitory processing in the vertical meridian: Evidence from elderly brain damaged patients. *Aging Brain* **2**, 100043 (2022).
60. Burgess, A. P. On the interpretation of synchronization in eeg hyperscanning studies: a cautionary note. *Front. Hum. Neurosci.* **7**, 881 (2013).
61. Trammell, J. P., MacRae, P. G., Davis, G., Bergstedt, D. & Anderson, A. E. The relationship of cognitive performance and the theta-alpha

power ratio is age-dependent: an EEG study of short term memory and reasoning during task and resting-state in healthy young and old adults. *Front. Aging Neurosci.* **9**, 364 (2017).
62. Rogala, J., Kublik, E., Krauz, R. & Wróbel, A. Resting-state eeg activity predicts frontoparietal network reconfiguration and improved attentional performance. *Sci. Rep.* **10**, 5064 (2020).
63. Vecchio, F. et al. Cortical connectivity and memory performance in cognitive decline: a study via graph theory from EEG data. *Neuroscience* **316**, 143–150 (2016).
64. Bouazzaoui, B. et al. Aging and self-reported internal and external memory strategy uses: the role of executive functioning. *Acta Psychol.* **135**, 59–66 (2010).
65. Stern, Y. Cognitive reserve in ageing and Alzheimer's disease. *Lancet Neurol.* **11**, 1006–1012 (2012).
66. Frankenmolen, N. L., Fasotti, L., Kessels, R. P. & Oosterman, J. M. The influence of cognitive reserve and age on the use of memory strategies. *Exp. Aging Res.* **44**, 117–134 (2018).
67. Scahill, R. I., Schott, J. M., Stevens, J. M., Rossor, M. N. & Fox, N. C. Mapping the evolution of regional atrophy in Alzheimer's disease: unbiased analysis of fluid-registered serial mri. *Proc. Natl. Acad. Sci. USA* **99**, 4703–4707 (2002).
68. Barnes, J. et al. A meta-analysis of hippocampal atrophy rates in Alzheimer's disease. *Neurobiol. Aging* **30**, 1711–1723 (2009).
69. Vemuri, P. & Jack, C. R. Role of structural MRI in Alzheimer's disease. *Alzheimer' Res. Ther.* **2**, 1–10 (2010).
70. Duara, R. et al. Medial temporal lobe atrophy on MRI scans and the diagnosis of Alzheimer disease. *Neurology* **71**, 1986–1992 (2008).
71. Contador, J. et al. Longitudinal brain atrophy and CSF biomarkers in early-onset Alzheimer's disease. *NeuroImage Clin.* **32**, 102804 (2021).
72. Aoki, Y. et al. Eeg resting-state networks in Alzheimer's disease associated with clinical symptoms. *Sci. Rep.* **13**, 3964 (2023).
73. Cai, S. et al. Altered functional connectivity of fusiform gyrus in subjects with amnestic mild cognitive impairment: a resting-state fMRI study. *Front. Hum. Neurosci.* **9**, 471 (2015).
74. Ma, D. et al. The fusiform gyrus exhibits an epigenetic signature for Alzheimer's disease. *Clin. Epigenet.* **12**, 1–16 (2020).
75. Aramadaka, S. et al. Neuroimaging in Alzheimer's disease for early diagnosis: a comprehensive review. *Cureus* **15**, e38544 (2023).
76. Alba, G., Vila, J., Rey, B., Montoya, P. & Muñoz, M. Á. The relationship between heart rate variability and electroencephalography functional connectivity variability is associated with cognitive flexibility. *Front. Hum. Neurosci.* **13**, 428262 (2019).
77. Imbimbo, C. et al. Heart rate variability and cognitive performance in adults with cardiovascular risk. *Cereb. Circul. Cogn. Behav.* **3**, 100136 (2022).
78. Idiaquez, J. & Roman, G. C. Autonomic dysfunction in neurodegenerative dementias. *J. Neurol. Sci.* **305**, 22–27 (2011).
79. Kong, S. D. et al. Heart rate variability during slow wave sleep is linked to functional connectivity in the central autonomic network. *Brain Commun.* **5**, fcad129 (2023).
80. Wu, S. et al. The neural dynamic mechanisms of asymmetric switch costs in a combined Stroop-task-switching paradigm. *Sci. Rep.* **5**, 10240 (2015).
81. Klug, M. & Gramann, K. Identifying key factors for improving ica-based decomposition of EEG data in mobile and stationary experiments. *Eur. J. Neurosci.* **54**, 8406–8420 (2021).
82. Gabard-Durnam, L. J. et al. Longitudinal eeg power in the first postnatal year differentiates autism outcomes. *Nat. Commun.* **10**, 4188 (2019).
83. Jia, H., Li, H. & Yu, D. The relationship between ERP components and eeg spatial complexity in a visual go/nogo task. *J. Neurophysiol.* **117**, 275–283 (2017).
84. Akaike, H. Factor analysis and aic. *Psychometrika* **52**, 317–332 (1987).
85. Schwarz, G. Estimating the dimension of a model. *The annals of statistics* **6**, 461–464 (1978).
86. van den Heuvel, M. P. et al. Proportional thresholding in resting-state fMRI functional connectivity networks and consequences for patient-control connectome studies: Issues and recommendations. *Neuroimage* **152**, 437–449 (2017).
87. Celka, P. Statistical analysis of the phase-locking value. *IEEE Signal Process. Lett.* **14**, 577–580 (2007).
88. Cui, G., Li, X. & Touyama, H. Emotion recognition based on group phase locking value using convolutional neural network. *Sci. Rep.* **13**, 3769 (2023).
89. Miles, S., Gnatt, I., Phillipou, A. & Nedeljkovic, M. Cognitive flexibility in acute anorexia nervosa and after recovery: a systematic review. *Clin. Psychol. Rev.* **81**, 101905 (2020).
90. Garba, A. E. et al. The influence of cognitive reserve on Alzheimer's disease progression. *Alzheimer Dement.* **17**, e054537 (2021).
91. Šneidere, K., Mondini, S. & Stepens, A. Role of eeg in measuring cognitive reserve: a rapid review. *Front. Aging Neurosci.* **12**, 249 (2020).
92. Steffener, J. & Stern, Y. Exploring the neural basis of cognitive reserve in aging. *Biochim. Biophys. Acta (BBA)-Mol. Basis Dis.* **1822**, 467–473 (2012).
93. Wei, K. et al. White matter hypointensities and hyperintensities have equivalent correlations with age and csf β-amyloid in the nondemented elderly. *Brain Behav.* **9**, e01457 (2019).
94. Plant, C. et al. Automated detection of brain atrophy patterns based on mri for the prediction of Alzheimer's disease. *Neuroimage* **50**, 162–174 (2010).
95. Rocca, M. A. et al. Brain mri atrophy quantification in ms: from methods to clinical application. *Neurology* **88**, 403–413 (2017).
96. Chan, Y. L. et al. Automated thresholding method for fnirs-based functional connectivity analysis: validation with a case study on Alzheimer's disease. *IEEE Trans. Neural Syst. Rehabilit. Eng.* **28**, 1691–1701 (2020).

Acknowledgements

The authors thank the study participants for their altruistic participation in this research. They also thank Dr. Astrid Suchy-Dicey for her support in submitting this manuscript, as well as Cathleen Molloy for revising the manuscript and handling some data, Shant Rising, and Rachel Woo for taking part in handling some data. Some data relied on in this study were derived from research performed at HMRI by Dr. Michael G. Harrington. This work was supported by the National Institute on Aging, National Institutes of Health (NIH) (grant numbers R56AG063857 and R01AG063857).

Author contributions

Conceived and designed the experiments: X.A.; performed the experiments: X.A.; neuropsychological data: A.N.; MRI data: HMRI Brain Imaging Center; Analyzed data: A.A.; Wrote the paper: A.A.; Behavioral analysis: D.W.; Heart rate variability analysis: M.K. and R.A.; Edited the paper: R.A., R.B., A.N., J.J.K., S.S., D.W., A.F., M.K., R.K., and X.A.; All authors contributed to the final manuscript.

Competing interests

The authors declare no competing interests.

Additional information

Supplementary information The online version contains supplementary material available at https://doi.org/10.1038/s42003-024-06673-w.

Correspondence and requests for materials should be addressed to Abdulhakim Al-Ezzi or Xianghong Arakaki.

Peer review information *Communications Biology* thanks Gleb Bezgin and the other, anonymous, reviewer(s) for their contribution to the peer review of this work. Primary Handling Editors: Christian Beste and Benjamin Bessieres. A peer review file is available.